

# Phenotype-Specific Bacterial Communities in the Cold-Water Coral *Lophelia pertusa* (Scleractinia) and Their Implications for the Coral's Nutrition, Health, and Distribution<sup>∇†</sup>

Sven C. Neulinger,<sup>1\*</sup> Johanna Järnegren,<sup>2</sup> Martin Ludvigsen,<sup>3</sup>  
Karin Lochte,<sup>1</sup> and Wolf-Christian Dullo<sup>4</sup>

Alfred Wegener Institute for Polar and Marine Research, Am Handelshafen 12, D-27570 Bremerhaven, Germany<sup>1</sup>;  
Norwegian Institute for Nature Research (NINA), NO-7485 Trondheim, Norway<sup>2</sup>; Department of Marine Technology,  
Norwegian University of Science and Technology (NTNU), NO-7491 Trondheim, Norway<sup>3</sup>; and Leibniz Institute of  
Marine Sciences (IFM-GEOMAR), East Shore Campus, Wischhofstrasse 1-3, D-24148 Kiel, Germany<sup>4</sup>

Received 1 August 2008/Accepted 6 October 2008

The pseudocolonial coral *Lophelia pertusa* (Scleractinia, Caryophylliidae) is a eurybathic, stenothermal cosmopolitan cold-water species. It occurs in two color varieties, white and red. *L. pertusa* builds vast cold-water coral reefs along the continental margins, which are among the most diverse deep-sea habitats. Microbiology of *L. pertusa* has been in scientific focus for only a few years, but the question of whether the coral holds a host-specific bacterial community has not been finally answered. Bacteria on coral samples from the Trondheimsfjord (Norway) were characterized by the culture-independent 16S rRNA gene-based techniques terminal restriction fragment length polymorphism and sequence analysis. *L. pertusa* revealed a high microbial richness. Clone sequences were dominated by members of the *Alpha*- and *Gammaproteobacteria*. Other abundant taxa were *Bacteroidetes*, *Actinobacteria*, *Verrucomicrobia*, *Firmicutes*, and *Planctomycetes*. The bacterial community of *L. pertusa* not only differed conspicuously from that of the environment but also varied with both the location and color variety of its host. Therefore, the microbial colonization cannot be termed “specific” *sensu stricto*. However, similarities to other coral-bacterium associations suggest the existence of “cold-water coral-specific” bacterial groups *sensu lato*. *L. pertusa*-associated bacteria appear to play a significant role in the nutrition of their host by degradation of sulfur compounds, cellulose, chitin, and end products of the coral's anaerobic metabolism. Some coral-associated microbes were regarded as opportunistic pathogens. Dominance of mixotrophic members of the *Rhodobacteraceae* in white *L. pertusa* could explain the wider dispersal of this phenotype by supplementary nutrition.

The pseudocolonial scleractinian coral *Lophelia pertusa* (L., 1758) belongs to the family Caryophylliidae. Though it is commonly referred to as a “deep-water” or “deep-sea” coral, this does not mean that it lives exclusively in deep oceanic water masses but describes the ability of the coral to thrive at greater water depths in a cold and dark environment. Occurrence of this species is rather defined by temperature (4 to 12°C; preferred range, 6 to 8°C), salinity (~35 to 37 PSU; 33 to 34 PSU in fjords), and dissolved oxygen (~3 to 5 ml · liter<sup>-1</sup>) (21). The coral grows from 39 m on the Tautra reef in the Norwegian Trondheimsfjord (27) down to 3,000 m in the Atlantic (60). In fact, *L. pertusa* inhabits shallow water only in Norwegian fjords (62) because of the low depth of the thermocline (22). *L. pertusa* is thus a rather eurybathic, but stenothermal, cold-water species, occurring in areas characterized by high biological production and vigorous hydrodynamic regimes (53). The species occurs in two color varieties: white (transparent) and red (also referred to as “pink”) (62). The question of whether these two phenotypes differ genetically is still open. Like all scleractinian corals from such environments, *L. pertusa* has no

algal endosymbionts that could enhance calcification, as in tropical waters. Nevertheless, *L. pertusa* is the dominant coral in the northeast Atlantic, forming giant carbonate mounds and reef patches along the continental margin from the North Cape to the Straits of Gibraltar. Its importance in reef-forming processes with respect to lithification was recently discussed by Noé et al. (47). *L. pertusa* is most abundant on the continental shelf in mid-Norway at a 200- to 400-m depth, with largest densities along the continental break and on edges of shelf-crossing trenches (19).

Interactions between warm-water corals and bacteria have been observed for decades, and there are copious examples where microbes do not just dwell passively on a coral but have noticeable beneficial and detrimental impacts on their host: many tropical corals ingest their own mucus (13), likely deriving nutrients from mucus-inhabiting bacteria (37). Hermatypic corals are prone to numerous bacterially induced diseases, among which are coral bleaching, black band disease, and white plague. Microbial surface fouling is another detrimental threat. Accordingly, many corals make use of antibiotic substances, the source of which could again be coral-associated bacteria themselves (34).

In recent years, molecular genetics has been increasingly applied to investigate the diversity and specificity of associations between bacteria and tropical reef corals. Culture-independent analysis of 16S rRNA genes revealed a richness in prokaryotic gene sequence patterns which rivals that of the

\* Corresponding author. Current address: Leibniz Institute of Marine Sciences (IFM-GEOMAR), West Shore Campus, Duesternbrooker Weg 20, 24105 Kiel, Germany. Phone: 49 431 600-1987. Fax: 49 431 600-4452. E-mail: sneulinger@ifm-geomar.de.

† Supplemental material for this article may be found at <http://aem.asm.org/>.

∇ Published ahead of print on 10 October 2008.

eukaryotic coral reef community. Not only are coral-associated bacteria different from water-column bacteria, but different coral species harbor dissimilar bacterial communities, even when physically adjacent; moreover, microbial patterns of the same coral species separated by time and space remain similar (54). This strongly suggests that coral-bacterium associations are nonrandom.

Though bacteria may be of great ecological significance for *L. pertusa*, as described above for warm-water scleractinians, only a few microbiological investigations have been made in recent years. Besides preliminary research on *L. pertusa*-associated bacteria (C. A. Kellogg, presented at the 2006 Ocean Sciences Meeting, Honolulu, HI, 20 to 24 February 2006; C. A. Kellogg and R. P. Stone, presented at the ASLO/TOS Ocean Research Conference, Honolulu, HI, 15 to 20 February 2004), Yakimov et al. (68) were the first to publish phylogenetic data on metabolically active microbes in Mediterranean specimens of this coral. By means of clone libraries derived from reverse-transcribed bacterial 16S rRNA, the authors showed that the coral shelters a microbial community different from that of dead corals, sediment, or surrounding water. Spatial variation of the bacterial community on *L. pertusa* from the Mingulay reefs in the Sea of the Hebrides was only recently observed by Großkurth (24). The author also reported evidence for both antimicrobial and growth-stimulating factors that may permit *L. pertusa* to influence the composition of its epibacterial community. Schöttner et al. (56) found that various parts (surface, skeleton, and mucus) of corals from in situ (fjord slope, Norway) and ex situ (maintenance tank) environments, ambient seawater, and proximal sediment each exhibit distinct community profiles. All of these studies show that living *L. pertusa* hosts special bacterial associations which are unlike those of the environment and probably are actively influenced by the coral. The associations appear to differ both with the partitioning of their host and with its habitat.

One prerequisite to call an observed coral-microbe association truly "specific" is spatial constancy. Thus, the next step in understanding the microbiology of *L. pertusa* is to compare coral-associated bacteria not only from different stations within the same geographic region but also from different geographic regions. Also, the existence of two color phenotypes in *L. pertusa* and their possible implications for microbial colonization must be taken into account. The present study aims at investigating the community structure and taxonomy of *L. pertusa*-hosted microbes with the following objectives: (i) comparison of the bacterial assemblages of *L. pertusa* from the Trondheimsfjord in Norway with those of the surrounding environment; this fjord is a high-latitude habitat comparable to those locations examined by the two latest studies (24, 56) but comprises one of the coral's shallowest occurrences (27) and features generally lower salinities than habitats along the continental margins; it was thus important to know whether *L. pertusa* from that region also harbors special assemblages of bacteria; (ii) determination of the variability of these bacterial assemblages with the coral's location in the Trondheimsfjord and with its color variety, respectively; and (iii) identification of the dominant bacterial groups associated with *L. pertusa* and their potential ecological role and comparison with the microbial community of Mediterranean *L. pertusa* (68).

Answers to these questions should illuminate the relations

between *L. pertusa* and its associated bacteria. In particular, the issue of whether this association is specific and implications for coral ecology (nutrition, health, and distribution) will be discussed.

Culture-independent approaches were employed to meet the proposed objectives: Objectives i and ii were accomplished by terminal restriction fragment length polymorphism (T-RFLP) (41) of the bacterial 16S rRNA gene. Objective iii was based on sequence analysis of 16S rRNA gene clones.

#### MATERIALS AND METHODS

**Sample area.** The Trondheimsfjord is located between 63°30' and 64°N and 9°30' and 11°30'E on the coast of mid-Norway. From the seaward Agdenes sill with a depth of 195 m, three consecutive basins stretch to the inland: the seaward basin, dropping to 617 m (the maximum depth of the fjord), separated from the large middle basin by the Tautra sill, and the Beitstadfjord (6, 29). High primary productivity within the fjord (55) favors the growth of zooplankton, which in turn serves as prey for *L. pertusa*. The coral occurs on the Agdenes reef complex in the seaward basin and on the Tautra sill. The Tautra reef complex is one of the world's shallowest cold-water coral reefs, reaching up to a depth of only 39 m below the sea surface (27).

**Sampling and fixation.** *L. pertusa* specimens were collected at three stations on the Tautra sill and in the seaward basin of the Trondheimsfjord on 20 and 21 October 2004: (i) 'Tautra' (geographic position, 63°35'34"N, 10°31'4"W; depth, 54 m; temperature, 9.6°C; salinity, 30.1 PSU), (ii) "Stokkberneset" (63°28'14"N, 9°55'8"W; 264 m; 8.1°C; 31.9 PSU), and (iii) "Røberg" (63°28'36"N, 9°59'43"W; 240 m; 8.1°C; 31.2 PSU). Station "Tautra" was characterized by silty sediment. The sites "Stokkberneset" and "Røberg," each with a rocky steep slope, lay about 30 km further southwest from "Tautra" at the transition to the sound connecting the seaward fjord basin and the Norwegian Sea. All sampling sites featured apparently healthy coral communities without signs of pollution or other direct human influence. Sampling was accomplished with the SUB-Fighter 7500 remotely operated vehicle (ROV) "Minerva" from the Norwegian University of Science and Technology, Trondheim. A landing net attached to the ROV served as a collection device. The net was cleaned after every sampling and also was rinsed by the strong water current during the descent of the ROV, so cross-contamination by remains of coral debris and mucus from the previous sampling was unlikely to occur. Moreover, sampling of coral parts that had been in contact with the net was avoided. Three colonies (white and red color varieties) were randomly collected at each station within a radius of about 10 m around the positions given above, and three living branches with three to five polyps were randomly taken per colony, for a total of 27 coral samples (15 white and 12 red). The branches were rinsed with sterile filtered seawater to remove loosely attached microbes from their surfaces and individually placed in sterile centrifuge tubes. All coral samples were incubated in sterile filtered MgCl<sub>2</sub> solution to anesthetize the coral polyps for 30 min. This was done for reasons of comparability with other coral samples taken for fluorescence in situ hybridization, where MgCl<sub>2</sub> was used to prevent the polyps from retraction (cf. reference 9). Samples were frozen at -20°C. Two samples of surrounding water (1 liter each) were collected about 1 m apart from the coral colonies at each station using a Niskin bottle that was attached to the ROV and disengaged remotely. Water samples were cooled to 4°C until their return to the laboratory at TBS (4 to 6 h) and filtered through polycarbonate Nuclepore membrane filters (0.2- $\mu$ m pore size, 47-mm diameter; Whatman). The filters were frozen at -20°C in small petri dishes. Two sediment samples were taken from the bases of two separate corals from station "Tautra" and stored at -20°C in sterile centrifuge tubes. It was not possible to collect sediment samples at the other two stations because of their rocky steep slope.

**DNA extraction.** Whole coral samples were pounded in liquid nitrogen with a mortar and pestle. To avoid carryover of DNA from consecutive sample treatments, tools were sterilized with 3 M HCl and neutralized with sterile filtered phosphate-buffered saline (pH 7.4). DNA was extracted from all sample types with the UltraClean soil DNA kit (Mo Bio). About 1 g of material (corals/sediment) and approximately one-eighth of the polycarbonate filter area (corresponding to about 125 ml of filtered seawater) were employed in each extraction, respectively. To minimize DNA shearing, the "alternative lysis method" proposed by the manufacturer (heating to 70°C instead of vortexing) was applied with a four-times-elongated incubation compared to the manufacturer's protocol.

**DNA amplification for T-RFLP.** PCR with template DNA from environmental and coral samples was conducted using the Phusion high-fidelity PCR kit (Finnzymes) according to the manufacturer's instructions and the *Bacteria*-specific primer 27f (5'-AGAGTTTGATCMTGGCTCAG-3') and universal primer 1492r (5'-GGTACCTTGTACGACTT-3'). This primer combination was chosen in order to amplify a broad range of bacterial 16S rRNA gene sequences. Archaea were not investigated in this study. Primers for T-RFLP were 5' labeled with the fluorescent dyes 6-carboxyfluorescein (27f) and VIC (1492r), respectively. The total reaction volume was 20  $\mu$ l, containing 6  $\mu$ l of template DNA. Since it was impossible to measure the amount of bacterial DNA in the extract (because eukaryotic DNA was present, too), the concentration of template DNA was adjusted to obtain clearly visible 16S rRNA gene bands on the agarose gel (~10 to 50 ng per band, estimated by ethidium bromide staining): undiluted DNA extract from coral samples or 1:400-diluted DNA extract from sediment and water samples. PCR conditions were 3 min at 98°C; 35 cycles of 10 s at 95°C, 30 s at 55°C, and 45 s at 72°C; and 1 terminal elongation step of 5 min at 72°C. The number of cycles had been adjusted to get a clear signal of coral-derived bacterial PCR products in gel electrophoresis. Since this cycle number was kept constant in the whole assay, the PCR bias as a systematic error remained comparable for all samples. PCR products were obtained from all coral samples except 1 red sample from station "Taura," resulting in 26 coral PCR products.

**Restriction digests.** PCR products were purified by excision from a 1% agarose gel in Tris-acetate-EDTA buffer and subsequent extraction with the NucleoSpin Extract II kit (Macherey-Nagel) and eluted from spin columns with 100  $\mu$ l elution buffer. They were concentrated by conventional isopropanol precipitation and resuspended with 30  $\mu$ l elution buffer. The PCR products were digested with two restriction endonucleases commonly used in T-RFLP, HhaI and AluI, respectively (New England Biolabs). Ten microliters of purified PCR product was mixed with 10  $\mu$ l of restriction enzyme master mix containing 5 U of the respective enzyme. Restriction reactions were incubated for 6 h at 37°C, followed by 20 min at 65°C to denature the enzyme.

**T-RFLP analysis.** Restriction products were purified by ethanol precipitation and resuspended in 12  $\mu$ l of Hi-Di formamide (Applied Biosystems). For determination of fragment lengths ("size calling"), a size standard mix was prepared containing 5.9  $\mu$ l of Hi-Di formamide and 0.1  $\mu$ l of the GeneScan 500 (ROX) size standard (Applied Biosystems) per sample. Six microliters of the size standard mix was merged with 6  $\mu$ l of the resuspended restriction product and denatured at 95°C for 5 min. Terminal restriction fragment (T-RF) signals were detected by capillary electrophoresis on an ABI Prism 310 genetic analyzer using the Pop-6 polymer in a 30-cm capillary (Applied Biosystems) under the following conditions: injection time, 15 s; injection/electrophoresis voltage, 15 kV; electrophoresis current, ~7 mA; gel temperature, 60°C; run time, 44 min. Electropherograms were analyzed using the program GeneScan v2.0.2 (Applied Biosystems).

**Statistics.** Peak data of T-RFs of between 30 and 500 nucleotides (nt) and signal intensities of  $\geq 50$  (arbitrary units) were exported as tabular data from the genetic analyzer. A data matrix was created from the combined HhaI and AluI peak data with samples as columns and peak positions (T-RF lengths) as rows. The area under each peak was used as a measure of T-RF abundance, standardized as a percentage of total peak area as described by Lukow et al. (43). Due to rounding errors and minor variations in size determination, the length of defined T-RFs varied by  $\pm 1$  nt among samples. Peaks were aligned within this range from their expected mean (cf. reference 45). Rows without T-RF data were deleted from the matrix. Two distance matrices were derived from the peak matrix employing (i) Manhattan distances and (ii) percent mismatch distances based on binary (presence-absence) data of peaks. Nonmetric multidimensional scaling (MDS) was applied to ordinate samples in three dimensions according to the distance matrices. Statistical analyses were performed with the following: (i) average peak numbers of the sample types and (ii) the three MDS dimensions as independent variables, and "sample type," "station," and "color variety" (of the coral samples) as categorical predictors. The Shapiro-Wilk W statistic was used to test the variables for normality. With normally distributed variables, a multivariate analysis of variances (MANOVA) was performed, followed by Duncan's test for post hoc evaluation of significant differences. For nonnormally distributed variables, nonparametric Kruskal-Wallis analysis of variance (ANOVA) was applied, combined with the Mann-Whitney U test for post hoc evaluation. All statistics were executed with the software program Statistica v6.1 (StatSoft).

**DNA amplification for cloning.** DNA extracts of all three stations were pooled according to environmental sample type (water/sediment) and color variety (corals). This pooling leveled differences in the DNA composition of the single samples. Thus, the following sequence analysis characterized the "average" bacterial community to be covered by DNA extraction from a respective sample type. In a first step, three parallel PCRs were conducted for each pool (water/sediment/white corals/red corals), each with a total reaction volume of 20  $\mu$ l,

containing 6  $\mu$ l (corals) or 1  $\mu$ l (water/sediment) of undiluted DNA extract as template. PCR was conducted using the Phusion high-fidelity PCR kit (Finnzymes) according to the manufacturer's instructions and primers 27f and 1492r. PCR conditions were 3 min at 98°C; 20 cycles of 10 s at 95°C, 30 s at 55°C, and 45 s at 72°C; and 1 terminal elongation step of 5 min at 72°C. PCR products of the three parallels were pooled and purified as described above (see "Restriction digests"). Elution from spin columns was done in a 25- $\mu$ l elution buffer. In a second step, the purified PCR products were reamplified in a total reaction volume of 50  $\mu$ l containing 6  $\mu$ l of template DNA (all samples). PCR conditions were as follows: 3 min at 98°C; 10 (water/sediment) or 20 (corals) cycles of 10 s at 95°C, 30 s at 55°C, and 45 s at 72°C; and 1 terminal elongation step of 5 min at 72°C. This two-step procedure was aimed at obtaining high-quality PCR products for cloning while reducing formation of chimeric sequences.

**Cloning.** PCR products were purified and precipitated as described above (see "Restriction digests"). Cloning was carried out using the Topo TA cloning kit for sequencing with One Shot TOP10 chemically competent *Escherichia coli* (Invitrogen). This kit was preferred for its high reliability, but it required DNA inserts with a 3' adenosine overlap for ligation with the cloning vector. Since the Phusion polymerase produces blunt-ended PCR products, a terminal deoxyadenosine had to be added to the 3' ends of the amplified DNA prior to ligation. For this purpose, the natural non-template-dependent terminal transferase activity of *Taq* polymerase was exploited: PCR products were incubated in 50  $\mu$ l of 1 $\times$  ThermoPol buffer (New England Biolabs) with 1 U of *Taq* DNA polymerase (New England Biolabs) and 200  $\mu$ M dATP (Roche) for 30 min at 72°C. After terminal adenosine addition, PCR products were purified and precipitated as described above (see "Restriction digests") and resuspended with 25  $\mu$ l elution buffer. Purified products were ligated into the vector, followed by transformation of competent *E. coli* according to the manufacturer's instructions. Cells were spread onto LB agar plates amended with kanamycin (the recipe is given in the Topo TA cloning kit manual) and grown at 37°C overnight. Clone-forming units were separated into 96-well plates filled with liquid LB medium and regrown at 37°C overnight. Cloned 16S rRNA gene inserts were reamplified with the primer pair T3/T7 (contained in the cloning kit). The total reaction volume was 45  $\mu$ l, containing 0.5  $\mu$ l of *E. coli* cell suspension, 1 U of *Taq* DNA polymerase (New England Biolabs), 0.1  $\mu$ M of each primer, 50  $\mu$ M of each deoxynucleoside triphosphate, and 1 $\times$  ThermoPol buffer. PCR conditions were as follows: 5 min at 95°C; 35 cycles of 10 s at 95°C, 30 s at 55°C, and 1 min at 72°C; and 1 terminal elongation step of 10 min at 72°C. Aliquots of 5  $\mu$ l (each) were taken from each PCR product and tested for their correct length (about 1,600 bp, including the T3 and T7 priming sites) by agarose gel electrophoresis.

**Sequencing.** PCR products from clones showing a correct length were sequenced at the Institute for Clinical Molecular Biology at Kiel University Hospital (Kiel, Germany). Purification of PCR products and the sequencing procedure were as described previously (23). Partial sequences were obtained by sequencing with primer 27f. For nearly complete sequences, PCR products were additionally sequenced with primer 1492r, followed by assembling of the two overlapping partial sequences.

**Phylogenetic analysis.** Sequence data were visually checked for quality issues. Putative chimeric sequences were detected and eliminated using the online tools Chimera Check v2.7, of the Ribosomal Database Project II release 8.1 (12), and the Bellerophon chimera detection program (28). The sequence classifier of Ribosomal Database Project II release 9 (<http://rdp.cmc.msu.edu/classifier/classifier.jsp>) (11) and BLAST (basic local alignment search tool [<http://www.ncbi.nlm.nih.gov/blast/blast.cgi>]) (1) were used for classification of the bacterial sequences and determination of closest relatives. The latter were obtained from the EMBL nucleotide sequence database (<http://www.ebi.ac.uk/embl>) (39). Data of sequences from this study, their closest relatives, and sequences of coral-associated bacteria from other studies were imported into a sequence library of ARB v2.5b (42) and aligned according to 16S rRNA secondary structure information. A positional mask was applied that allowed only unambiguously alignable sequence positions in all subsequent phylogenetic assays. This mask comprised *E. coli* 16S rRNA positions (8) 28 to 68, 101 to 183, 220 to 451, 480 to 838, 848 to 1003, 1037 to 1134, 1140 to 1440, and 1461 to 1491. Aligned sequences were incorporated into the phylogenetic "backbone" tree of the ARB library, consisting of more than 52,000 sequences, using maximum parsimony as the inference method. Sequences were grouped into operational taxonomic units (OTUs) if the proportion of identical sequence positions shared between any two of them was  $\geq 97\%$ , which corresponds approximately to affiliation with the same species (61). A rarefaction analysis was conducted using the program aRarefactWin by S. M. Holland (<http://www.uga.edu/~strata/software/>). Theoretical coverage of microbial diversity in the different sample types was estimated from rarefaction curves with the equation  $y = a \times (1 - e^{-b \times x^c})$  (66), where  $x$  is the sample size,  $y$  the observed number of OTUs, and  $a$  the number of OTUs to be

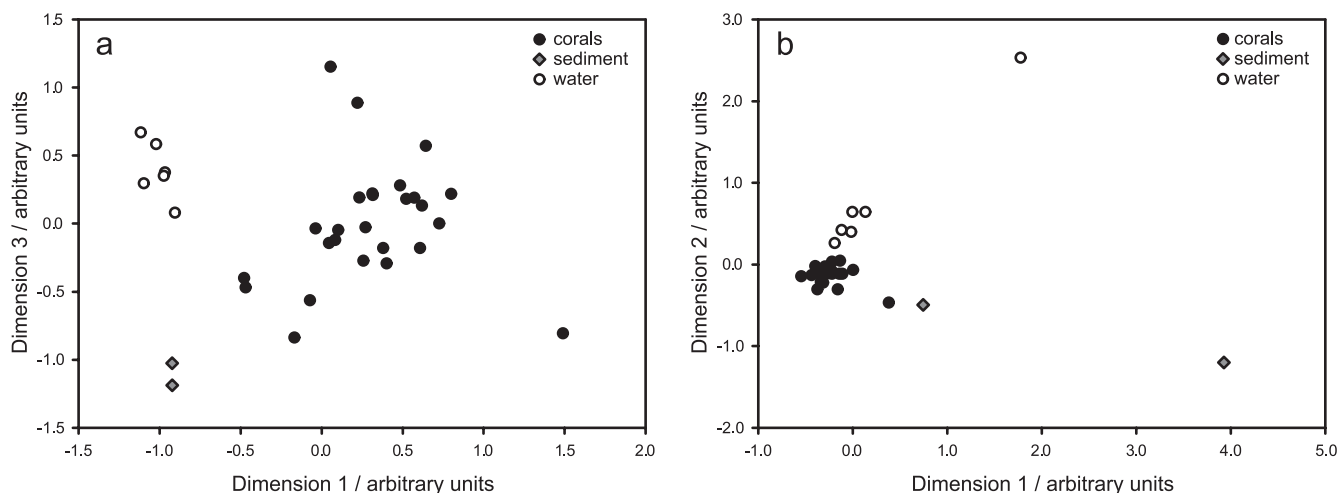


FIG. 1. MDS ordination of coral (26 data points), sediment (2 data points), and water samples (6 data points). Ordination was based on Manhattan distances (a) and percent mismatch distances (b) derived from the T-RF peak matrix. For clearness, of the three calculated MDS dimensions only the two with the most conspicuous differences were plotted. The stress value for dimensional downscaling was 0.10 (a) or 0.05 (b), respectively.

expected with an infinite sample size. (*b* and *c* are additional parameters to fit the curve shape.) A maximum-likelihood tree with sequences of interest was calculated with 100 bootstrap replicates using the program PHYML (25). To ensure clearness and reliability of this tree, a subset of 133 sequences from the initial ARB alignment was used. This subset contained only reference sequences of relevant OTUs from this study, sequences of coral-associated bacteria from other studies, and EMBL reference sequences. An OTU was considered “relevant” if it (i) comprised at least two sequences from this study that were not from water or sediment clones or (ii) was related to a sequence of a coral-associated bacterium from another study. The corresponding subset of the ARB “backbone” tree was used as a starting tree in PHYML, sustaining topology and branch lengths. The most appropriate model of nucleotide substitution for the maximum-likelihood calculation was determined using the program ModelGenerator v0.84 (32). A detailed phylogeny for classification of members of the *L. pertusa*-hosted *Mycoplasmataceae* was calculated with maximum likelihood as described above and with maximum parsimony and 1,000 bootstrap replicates using PHYLIP DNAPARS v3.6a3 (18) implemented in ARB.

**Nucleotide sequence accession numbers.** Reference clone sequences of all OTUs from *L. pertusa* samples and all clone sequences from water and sediment samples obtained in this study were deposited in the EMBL nucleotide sequence database (39) under accession numbers AM911346 to AM911622.

## RESULTS

**Comparison of coral and environmental samples.** T-RFLP analysis of this study yielded data sets for 26 coral, 6 water, and 2 sediment samples. A total of 517 different electropherogram T-RF lengths were observed. Overlay plots of electropherograms from the three sample types are shown in Fig. S1 in the supplemental material for restriction enzymes HhaI (see Fig. S1a) and AluI (see Fig. S1b) in combination with primer 27f. This figure gives an impression of what the raw data obtained from the genetic analyzer looked like. However, it neither provides a detailed view due to the limited resolution of the graphic nor allows direct comparison of relative peak intensities. Analyses were therefore solely conducted on the peak matrix. Comparative values for T-RF profiles of the different sample types are summarized in Table S1 in the supplemental material. In the peak matrix, 167 (32.3%) peaks belonged exclusively to corals, while the others were shared with sediment (34 peaks [6.6%]), water (49 peaks [9.5%]), or both (78

peaks [15.1%]), summing up to a total of 161 shared peaks (31.1%). The average number of peaks per sample was highest for sediment (150.5), followed by water (83.8), red (54.3), and white (39.4) coral samples. Significance of these differences was tested by Kruskal-Wallis ANOVA and the Mann-Whitney U test, because the distribution of average peak numbers deviated from normality. Kruskal-Wallis ANOVA indicated significant differences between average peak numbers of the respective sample types ( $P < 0.01$ ). However, the divergence between average peak numbers of red and white coral samples was insignificant according to the Mann-Whitney U test.

Nonmetric multidimensional scaling (MDS) is used in data visualization for exploring similarities or dissimilarities between items. In this case, the items were coral and environmental samples and the measure of dissimilarity was the Manhattan or percent mismatch distance between any pair of samples based on their T-RFLP peak patterns. Manhattan distance is more robust to outliers than the conventional Euclidean distance measure in the case of normalized peak areas, while the percent mismatch measure is particularly suited for binary (presence-absence) data. For clearness, of the three dimensions calculated by MDS, only the two with the most conspicuous differences were plotted in the following diagrams. Coral, water, and sediment samples of all stations were clearly separated from each other by MDS based on normalized peak areas (Fig. 1a) (stress: 0.10). Data points clustered closely together within their respective sample type with no overlap between different sample types. This separation of coral, water, and sediment samples was corroborated by MANOVA ( $P < 0.00$ ). A similar picture was given by MDS based only on binary peak data (Fig. 1b) (stress: 0.05), though this analysis led to greater scattering compared to MDS based on normalized peak areas. The two more remote sample points in question (one from water and one from sediment) belonged to samples with above-average peak numbers in their T-RFLP profiles. For binary peak data the same clear separation of

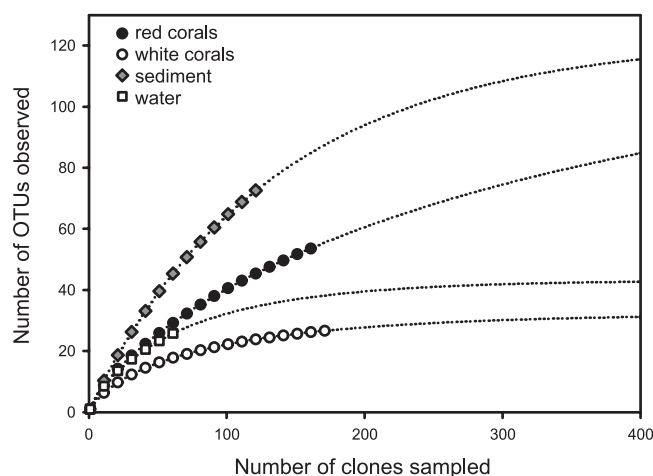


FIG. 2. Rarefaction analysis. The expected number of OTUs is plotted against the number of analyzed clones from red and white *L. pertusa*, sediment, and water. Dotted lines mark the extrapolations of the respective rarefaction curves according to the equation  $y = a \times (1 - e^{-b \times x^c})$  (66), where  $x$  is the sample size,  $y$  the observed number of OTUs, and  $a$  the number of OTUs to be expected with an infinite sample size, which represents the maximum expectable OTU richness.

sample types as for normalized peak data was confirmed by Kruskal-Wallis ANOVA ( $P < 0.00$  for dimensions 1 and 2).

**Differences between coral samples.** For analysis of coral samples, T-RFs were divided into two categories: (i) “rare” peaks occurring in less than one-third ( $<9$ ) of the coral samples (291 T-RFs) and (ii) “consistent” peaks occurring in at least one third ( $\geq 9$ ) of the coral samples (37 T-RFs). Though only about one out of nine coral-derived T-RFs was consistent according to this definition, the second category comprised all dominant peaks (i.e., peaks with highest relative abundance values; see Fig. S2 in the supplemental material). MDS dimensions derived from relative abundances of rare peaks (stress: 0.12) (not shown) deviated considerably from normal distribution. Kruskal-Wallis ANOVA revealed significant differences between stations in dimension 1 ( $P < 0.01$ ). Pairwise comparison by the Mann-Whitney U test denoted the differences between stations 1 and 2 ( $P = 0.03$ ) and between stations 2 and 3 ( $P < 0.01$ ) to be significant. The effect of “color variety” was insignificant. MDS data of consistent peaks (stress: 0.09; not shown) were approximately normally distributed. With two-way MANOVA, the predictor “station” accounted for a significant difference between corals from different sampling sites ( $P = 0.03$ ). Post hoc comparison with Duncan’s test revealed significant differences between stations 1 and 2 ( $P < 0.01$ ). In addition, dissimilarities between T-RFLP profiles from corals of different colors, denoted by the predictor “color variety,” also were significant ( $P = 0.05$ ). The crossover effect “station”  $\times$  “color variety,” which was evaluated by two-way MANOVA, was insignificant. Corresponding analyses were carried out with MDS dimensions based on rare binary peak data (stress: 0.00) and dominant binary peak data (stress: 0.15) (not shown). Since variables considerably deviated from normal distribution in both cases, Kruskal-Wallis ANOVA and the Mann-Whitney U test were employed to test differences between samples. In consideration of rare binary T-RF data,

the predictor “station” accounted for significant differences between coral samples in dimensions 1 ( $P = 0.02$ ) and 3 ( $P = 0.04$ ). Post hoc comparisons yielded significant differences between stations 1 and 2 (dimension 3;  $P < 0.01$ ) and between stations 2 and 3 (dimension 1;  $P = 0.02$ ). The effect of “color variety” was insignificant. No significant differences were observed for any of the two predictors in consideration of dominant binary T-RF data.

**Sequence analysis.** A total of 536 16S rRNA gene sequences passed quality checks and were subjected to phylogenetic analysis: 177 from white corals, 163 from red corals, 71 from water, and 125 from sediment. Lengths of partial sequences ranged from 294 nt (one instance) to 902 nt (average, 765 nt). Twelve nearly complete sequences from selected bacterial OTUs were retrieved to increase the data basis for phylogenetic calculations. These sequences were 1,318 nt to 1,421 nt long (average, 1,374 nt) and denominated by the suffix “full.” Based on 97% sequence similarity, the number of OTUs found in the respective sample types were 27 (white corals), 54 (red corals), 28 (water), and 74 (sediment). Rarefaction analysis (Fig. 2) assigned highest bacterial OTU richness to the sediment, followed by red *L. pertusa*, water, and white *L. pertusa*. Consequently, theoretical coverage of total bacterial diversity was highest in white *L. pertusa* (83.2%), followed by water (64.7%), sediment (60.3%), and red *L. pertusa* (42.1%). Table 1 summarizes these properties of the sequence library. Affiliation with bacterial phyla and classes (in case of *Proteobacteria*) and relative abundances of 16S rRNA gene sequences from corals, water, and sediment are shown in Fig. 3. Qualitative and quantitative differences of the large-scale bacterial community compositions between coral, water, and sediment samples are visible at first sight. Sequences assigned to the phylum *Proteobacteria* constituted the largest fraction, not only in water and sediment but also in both coral color varieties (64% in white and 50% in red *L. pertusa*). In either case, this fraction was dominated by the classes *Alpha-* and *Gammaproteobacteria*. Other major taxa (relative abundance,  $\geq 10\%$ ) occurring on both coral phenotypes were *Actinobacteria*, *Verrucomicrobia*, *Firmicutes*, and *Planctomycetes*. Some minor taxa (relative abundance,  $<10\%$ ) were exclusively found on either color variety, namely, candidate division TM7 on white *L. pertusa* and *Deltaproteobacteria* as well as *Bacteroidetes* on red *L. pertusa*. A small group of cyanobacterial sequences was found on both coral color varieties but not in the water. Detailed analysis on the OTU level revealed that despite the number of phyla and classes shared among coral color variations, white and red *L. pertusa* had only 12 OTUs in common. This equals a mere 16% of the combined bacterial richness of 75 OTUs for both coral

TABLE 1. Properties of the sequence library<sup>a</sup>

Sample type	No. of clones	No. of OTUs	Coverage (%)
White corals	177	27	83.2
Red corals	163	54	42.1
Water	71	28	64.7
Sediment	125	74	60.3

<sup>a</sup> For all sample types, the following values are given: number of analyzed clones, number of OTUs based on 97% sequence similarity, and theoretical coverage of total bacterial richness estimated by rarefaction analysis.

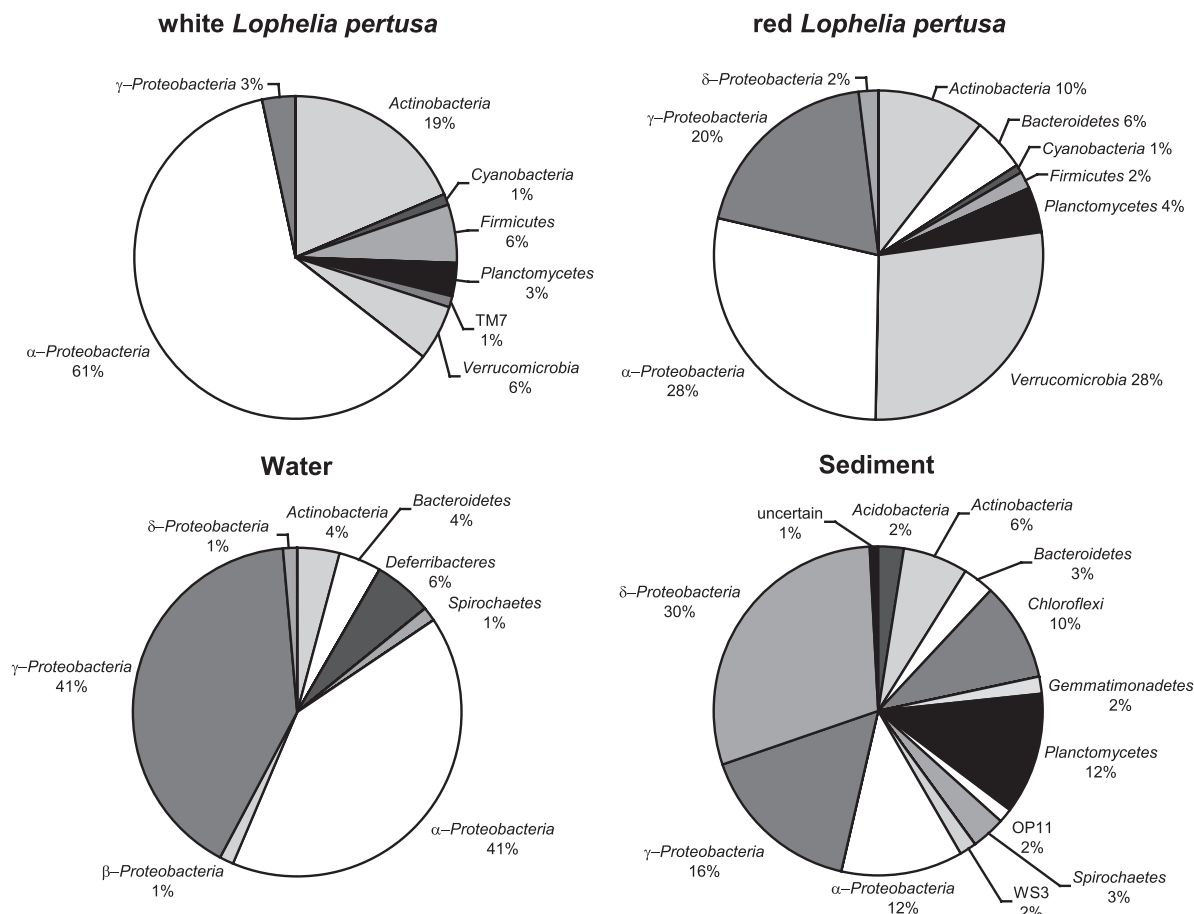


FIG. 3. Affiliation with bacterial phyla and classes (*Proteobacteria*) and relative abundances of 16S rRNA gene sequences. Data are given separately for red and white *L. pertusa*, water, and sediment.

color varieties. Commonalities between corals and the environment were confined to the class *Gammaproteobacteria*, where three OTUs were common to corals and seawater and one OTU was shared between corals and sediment.

A phylogeny of 133 reference sequences of relevant OTUs is shown in Fig. 4. These OTUs (i) comprised at least two sequences from this study that were not from water or sediment clones or (ii) were related to a sequence of a coral-associated bacterium from another study. The phylogenetic tree was based on maximum-likelihood calculation according to the generalized time-reversible model of nucleotide substitution with invariant sites and gamma distribution. The phylogeny was consistent with high-level bacterial taxonomy and reliably assorted sequences within their respective clusters as confirmed by bootstrapping. Relevant OTUs affiliated with eight bacterial phyla (*Proteobacteria*, *Bacteroidetes*, *Firmicutes*, *Cyanobacteria*, candidate division TM7, *Actinobacteria*, *Verrucomicrobia*, and *Planctomycetes*). Several sequences published by Yakimov et al. (68) belonged to three additional phyla (*Gemmatimonadetes*, *Acidobacteria*, and *Nitrospira*) that were associated only with Mediterranean *L. pertusa* and were not found on the specimens from the Trondheimsfjord.

Details on these bacterial groups are presented below, emphasizing microbes of potential significance for the ecology of

*L. pertusa*. Taxonomic classification below the phylum/class level is given for *L. pertusa*-associated OTUs as far it could be reliably determined. For all database sequences, accession numbers and similarities to *L. pertusa*-originating sequences are stated in parentheses. In cases with no overlap between an *L. pertusa*-originating sequence and a database sequence, the similarity to the closest common relative was determined instead.

The *Alphaproteobacteria* contained most of the coral-derived OTUs from this study. Within this class, sequences of the family *Rhodobacteraceae* constituted the largest subcluster, dominated by clones from white *L. pertusa*. In particular, 65 identical sequences from white *L. pertusa* (37% of all white *L. pertusa*-hosted sequences; reference, D05\_CW03\_full) showed high similarity to sequences from two bacterial strains, DIII4\* (accession no. AF254106; 98%) and EI1\* (AF254105; 98%) (asterisks are part of the clone names) isolated from North Atlantic continental slope sediments at a 1,500-m depth (64). These strains are capable of thiosulphate ( $S_2O_3^{2-}$ ) oxidation. A sequence of presumably the same bacterial species (accession no. DQ395503; 98%) had also been found on deep-sea octocorals of the family Isididae, so-called “bamboo corals” (*Octocorallia*, *Gorgonacea*, *Isididae*; scientific species names not provided) growing on seamounts in the Gulf of Alaska

a

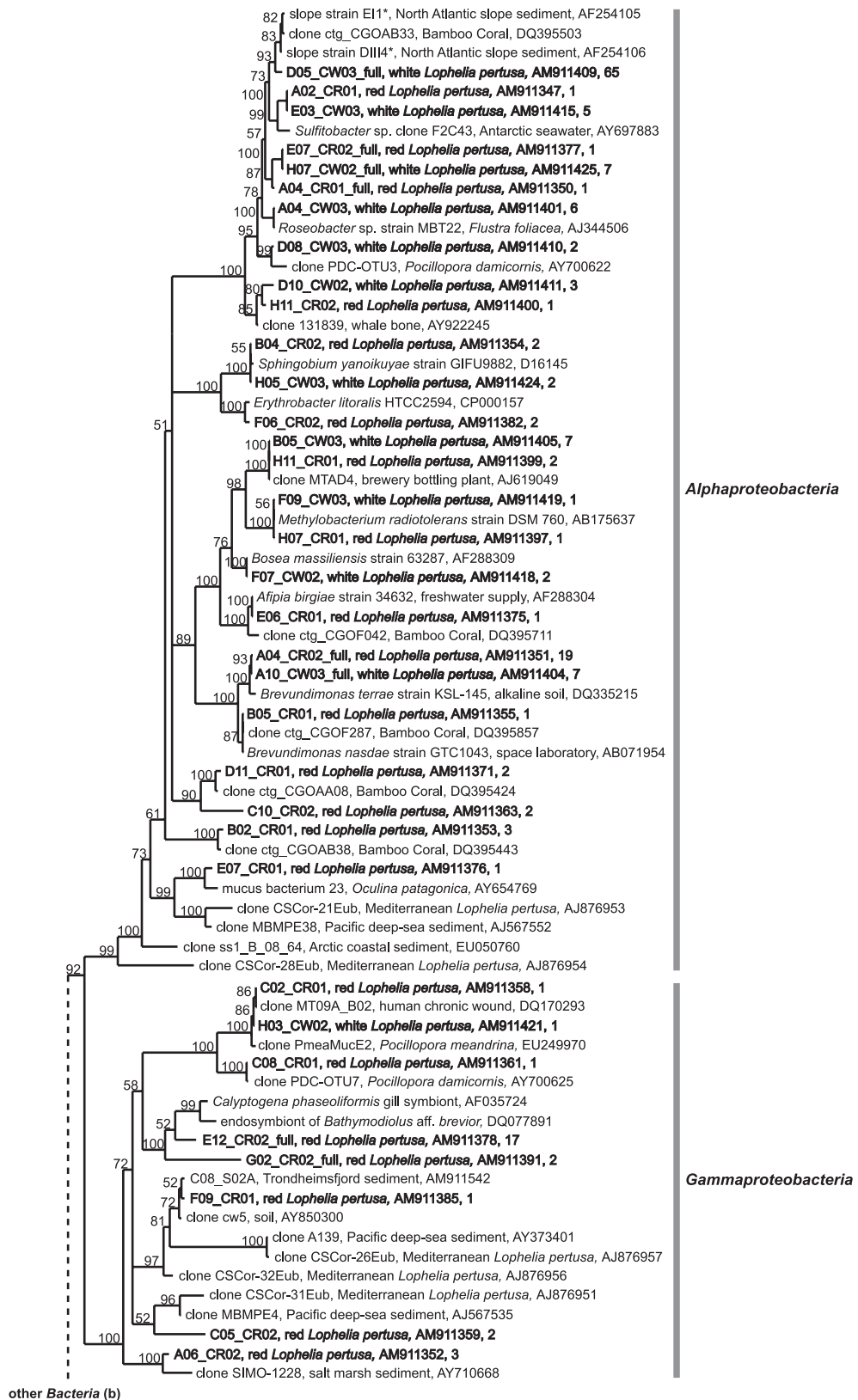


FIG. 4. Maximum-likelihood tree subdivided into proteobacterial (a) and other bacterial (b) relevant OTUs from white and red Norwegian *L. pertusa* (bold type), Mediterranean *L. pertusa*, other corals, and reference organisms. For each sequence, its name, source (if available), and EMBL accession number and the number of similar clones with a 97% identity cutoff (sequences from this study) are given. Bootstrap proportions of  $\geq 50\%$  from 100 resamples are shown next to the clusters they support. Branches leading to clusters with bootstrap proportions of  $< 50\%$  are collapsed. The sequence of *Aquifex aeolicus* (AE000709) was used to root the tree. The shaded box in panel b marks a group of coral-inhabiting *Mycoplasmataceae* (see Fig. 5). Scale bar (a and b, bottom left), 0.10 nucleotide substitutions per alignment position.

**b**

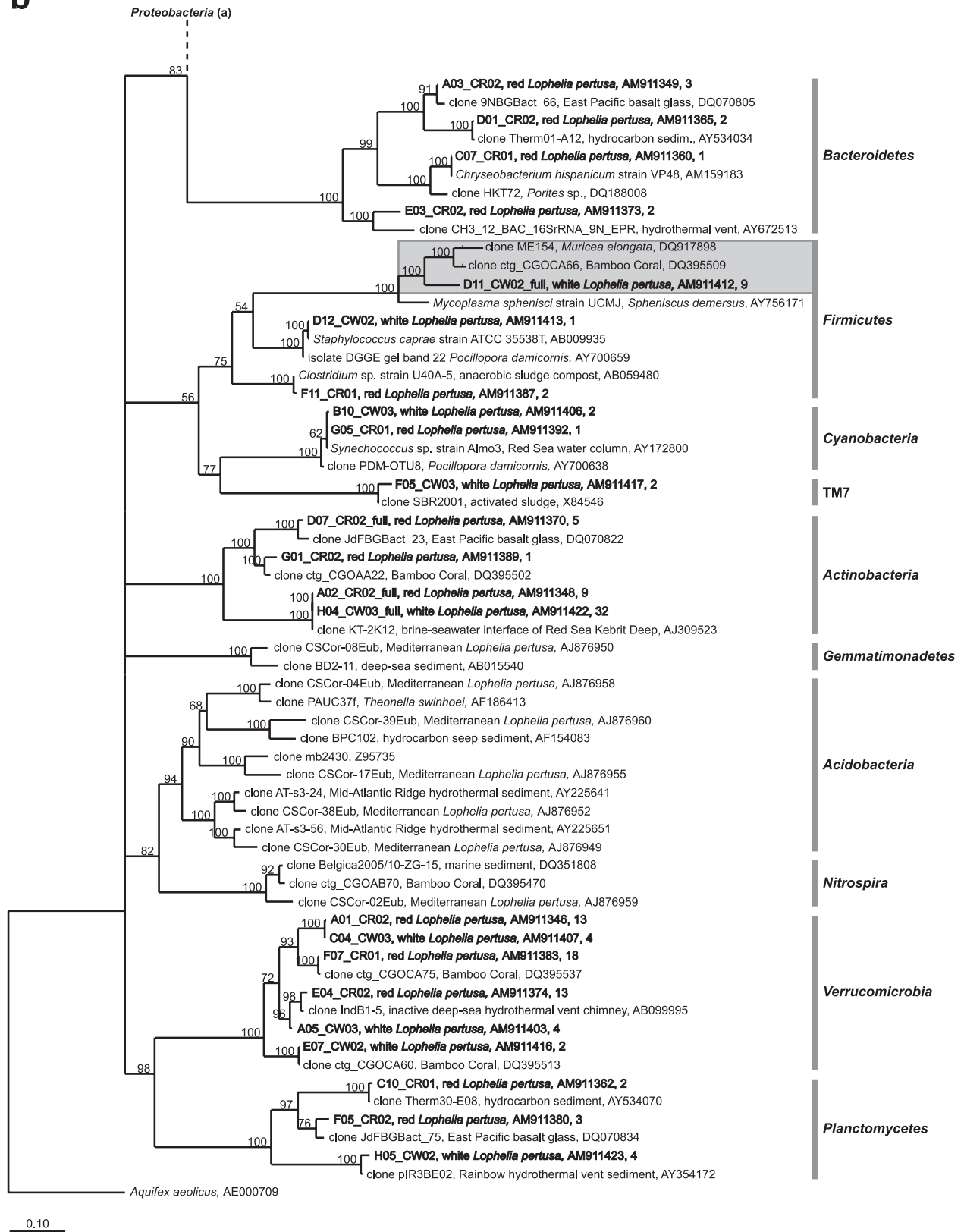


FIG. 4—Continued.

(50). Several bacterial sequences from red *L. pertusa* within the *Alphaproteobacteria* affiliated with sequences from other coral-associated bacteria: D08\_CW03 (*Rhodobacteraceae*) was similar to a sequence (accession no. AY700622; 97%) associated with the tropical scleractinian coral *Pocillopora damicornis* (*Astrocoeniina*, *Pocilloporidae*) (7). Several sequences from *L. pertusa* associated with sequences from *Isididae* (accession numbers DQ395xxx): E06\_CR01 (*Afipia* sp.) with accession no. DQ395711 (98%); a cluster of 19 sequences from red and 7 sequences from white *L. pertusa* (references, A04\_CR02\_full and A10\_CW03\_full) and B05\_CR01 from red *L. pertusa* (all *Brevundimonas* species) with accession no. DQ395857 (97%, 98%, and 100%, respectively); 2 sequences (reference, D11\_CR01; *Rhizobiales*) with accession no. DQ395424 (99%); and 3 sequences (reference, B02\_CR01; unclassified alphaproteobacteria) with accession no. DQ395443 (99%). E07\_CR01 (*Rhodospirillaceae*) associated with a sequence (accession no. AY654769; 97%) obtained from the mucus of the shallow-water scleractinian *Oculina patagonica* (*Faviina*, *Oculinidae*) (O. Koren and E. Rosenberg, unpublished). Other alphaproteobacterial sequences from both white and red *L. pertusa* (F09\_CW03 and H07\_CR01) were virtually identical to that of *Methylobacterium radiotolerans* (AB175637; 100% in both cases) (31); a larger sister-cluster of seven sequences from white and two from red corals (references, B05\_CW03 and H11\_CR01) also belonged to the genus *Methylobacterium*.

The *Gammaproteobacteria* cluster was dominated by bacterial sequences from red *L. pertusa*. The largest group of them comprised 17 sequences with reference E12\_CR02\_full (unclassified *gammaproteobacteria*). This cluster showed closest relatedness to thiotrophic endosymbionts of the two deep-sea mussels *Calyptogena phaseoliformis* (accession no. AF035724; 94%) (49) and *Bathymodiolus* aff. *brevior* (DQ077891; 93%) (44). Two other sequences (reference, G02\_CR02\_full) belonged to the same cluster but were more distantly related to the above-mentioned database sequences (88% and 87%, respectively). Additional BLAST searches were conducted with references E12\_CR02\_full and G02\_CR02\_full, respectively (data not shown). Out of each 100 hits for the respective reference, about 60 sequences originate from sulfur-oxidizing symbiotic bacteria hosted by the above-mentioned species and other species of deep-sea mussels. Even sequences of free-living bacteria with lowest similarity values are clearly related to thiotrophy or hydrothermal activity, respectively. Sequences C02\_CR01 from red corals and H03\_CW02 (both *Shigella* species) from white corals were almost identical to a clone sequence (accession no. DQ170293; 100% in both cases) obtained from a human wound (D. N. Frank, A. Wysocki, D. D. Specht-Glick, A. Rooney, R. A. Feldman, A. L. St. Amand, N. R. Pace, and J. Trend, unpublished). Sequence C08\_CR01 (*Vibrio* sp.) from red *L. pertusa* was identical to that of another bacterium from the tropical scleractinian *P. damicornis* (accession no. AY700625; 100%). A clone of probably the same species has also been identified on mucus of the scleractinian coral *Pocillopora meandrina* (*Astrocoeniina*, *Pocilloporidae*) (accession no. EU249970; 99% to both *L. pertusa*-derived sequences) (M. D. Speck, S. P. Donachie, and S. K. Davy, unpublished).

The *Bacteroidetes* cluster consisted exclusively of sequences associated with red *L. pertusa*. Sequence C07\_CR01 (*Chryseobacterium* sp.) was phylogenetically related to sequence

DQ188008, obtained from the shallow-water scleractinian *Porites* species (*Fungiina*, *Poritidae*) from the Arabian Sea (30). There was no overlap between C07\_CR01 and DQ188008, but DQ188008 was 96% similar to *Chryseobacterium hispanicum* AM159183, which in turn showed 100% similarity to C07\_CR01.

The *Firmicutes* cluster comprised mostly sequences from white *L. pertusa* that were closely related to bacteria from other corals: D12\_CW02 (*Staphylococcus* sp.) affiliated with a sequence from *P. damicornis* (accession no. AY700659; no overlap, 99% to *Staphylococcus caprae* AB009935), and two sequences (reference, F11\_CR01; *Clostridiaceae*) were highly similar to an isolate from an enriched anaerobic microbial community (AB059480; 100%) (67). A cluster of nine sequences (reference, D11\_CW02\_full; *Mycoplasmataceae*) were only distantly related to the next cultivated relative, *Mycoplasma sphenisci* (AY756171; 89%) (20). They formed a separate cluster with bacteria associated with *Isididae* (DQ395509; 91%) and the Caribbean coral *Muricea elongata* (*Octocorallia*, *Gorgonacea*, *Plexauridae*) (DQ917898; 90%) (L. K. Ranzer, P. F. Restrepo, and R. G. Kerr, unpublished), which is marked by a shaded box in Fig. 4b. To determine the exact phylogenetic position of this coral-related subcluster, an additional tree (Fig. 5) was constructed with both maximum likelihood and maximum parsimony. The model of nucleotide substitution for maximum-likelihood calculations was GTR+I+G. Several 16S rRNA gene sequences of >1,300 nt in length of cultivated and uncultivated relatives were used as an outgroup. (Note that for the *Mycoplasmataceae*, taxonomy is not always congruent with phylogeny). Calculations placed the coral-related *Mycoplasmataceae* in the *Mycoplasma hominis* group. The reliability of this classification was confirmed by high bootstrap proportions for both calculation methods throughout the tree and particularly within the coral-related sequence cluster.

Cyanobacteria were found in both white and red *L. pertusa* (references, B10\_CW03 and G05\_CR01, respectively) and belonged to the genus *Synechococcus*. Bacteria of the same genus are hosted by the tropical reef coral *P. damicornis* (accession no. AY700638; similarity, 98% to both references).

Candidate division TM7 had two representatives from white *L. pertusa* (reference, F05\_CW03) that were 98% similar to the partial 16S rRNA sequence X84546, obtained from activated sludge (5).

The *Actinobacteria* cluster comprised sequences from both white and red *L. pertusa*. Sequence G01\_CR02 (unclassified *Actinobacteria*) affiliated with a sequence from *Isididae* (accession no. DQ395502; 97%). A large subcluster consisting of nine sequences from red *L. pertusa* (reference, A02\_CR02\_full) and 32 sequences from white *L. pertusa* (reference, H04\_CW03\_full; *Propionibacterium acnes*) was identical with sequence AJ309523 (100%), obtained from the brine-seawater interface of Kebrit Deep in the Red Sea (17).

In the *Verrucomicrobia*, a large proportion of sequences affiliated with sequences from *Isididae* (accession numbers DQ3955xx), 18 sequences (reference, F07\_CR01; *Rubritalea* species), were identical to the DQ395537 sequence (100%); a large sister cluster of 13 sequences from red and 4 sequences from white *L. pertusa* (references, A01\_CR02 and C04\_CW03) belonged to the same genus, *Rubritalea* (92% similarity to the

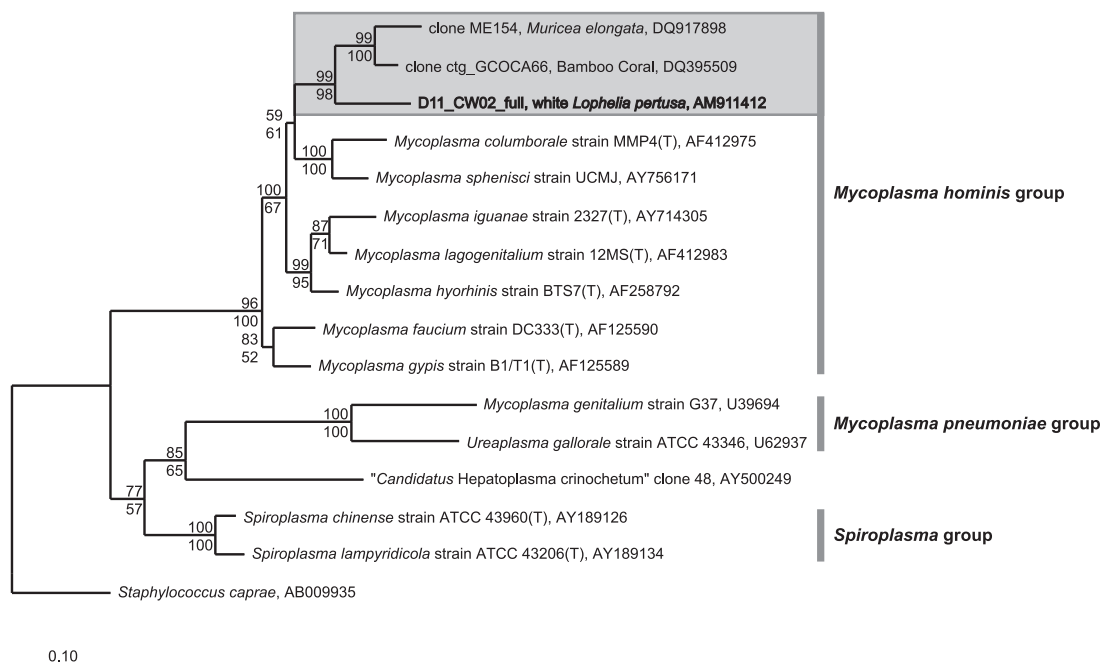


FIG. 5. Maximum-likelihood tree of *L. pertusa*-inhabiting *Mycoplasmataceae* with sequences of cultivated and uncultivated relatives. The coral-related sequences are marked by a shaded box, and reference sequence D11\_CW02\_full from this study is in bold. For each sequence, its name, source (if a clone), and EMBL accession number are given. "(T)" behind the strain designation denotes a type strain. Bootstrap proportions from 100 resamples for maximum likelihood (upper value) and 1,000 resamples for maximum parsimony (lower value) are shown next to the clusters they support. The sequence of *Staphylococcus caprae* (AB009935) was used to root the tree. The scale bar (bottom left) denotes 0.10 nucleotide substitutions per alignment position.

DQ395537 sequence); two sequences (reference, E07\_CW02; *Verrucomicrobiales*) were identical with the DQ395513 sequence (100%). Another subcluster consisted of 13 sequences from red *L. pertusa* (reference, E04\_CR02) and 4 sequences from white *L. pertusa* (reference, A05\_CW03) (both *Rubritalea* species) that showed high similarity to sequence AB099995 (98% and 97%, respectively) of an uncultured bacterium from inactive deep-sea hydrothermal vent chimneys (63).

The *Planctomycetes* cluster comprised coral-associated sequences of both white and red *L. pertusa*, too. Four sequences from white *L. pertusa* (reference, H05\_CW02; *Planctomyces* sp.) showed closest relatedness to sequence AY354172 (98%) of an uncultured bacterium from sediment of Rainbow vent field on the Mid-Atlantic Ridge (46).

Bacteria from Mediterranean *L. pertusa* (accession numbers AJ8769xx) (68) did not show direct affiliation with Norwegian *L. pertusa*-hosted bacteria. Yakimov et al. (68) sequenced their bacterial clones partially from the 3' end, while 5' partial sequencing was used for most clones in the present study. Straight comparison was thus impeded by missing sequence overlap. Still, Mediterranean and Norwegian sequences did not even have common relatives from the online database in most cases, except for two instances, the AJ876951 sequence and two sequences from red *L. pertusa* (reference; C05\_CR02; *Gammaproteobacteria*) that both clustered with a clone obtained from deep-sea sediment (accession no. AJ567535; 97% and 90%, respectively); sequences AJ876956 and F09\_CR01 (*Gammaproteobacteria*) from red *L. pertusa* showed 96% and 99% similarity, respectively, to an uncultured soil bacterium (accession no. AY850300). However, F09\_CR01 was the one

sequence closely related to a sequence from Trondheimsfjord sediment (C08\_S02A; 99%), and the corresponding bacterium was thus not exclusively confined to *L. pertusa* in its Norwegian habitat. The AJ876953 sequence from Mediterranean *L. pertusa* was in a sister clade of E07\_CR01 (*Alphaproteobacteria*, *Rhodospirillaceae*) associated with a sequence originating from *O. patagonica* (see above). Several sequences from Mediterranean *L. pertusa* affiliated with clones from hydrocarbon seep or hydrothermal sediments.

The clusters *Gemmatimonadetes*, *Acidobacteria*, and *Nitrospira* exclusively consisted of sequences from Mediterranean *L. pertusa*. Sequence AJ876950 had been classified as a member of *Actinobacteria* in the original study and was reclassified as a member of the *Gemmatimonadetes* in the present study. Within the *Nitrospira* cluster, sequence AJ876959 (*Nitrospira* sp.) showed moderate relatedness to another sequence from an isidid coral (DQ395470; 95%). The above-mentioned affiliation with deep-sea and seep-related bacteria was most distinct within the *Gemmatimonadetes* and *Acidobacteria*.

## DISCUSSION

**Differences in bacterial assemblages of *L. pertusa*.** The bacterial associations in Norwegian *L. pertusa* from the Trondheimsfjord were found to be highly diverse and differed from microbial communities of the environment, which is in accordance with results of other studies (24, 56, 68). T-RFLP fingerprinting was used to compare microbial communities in *L. pertusa* to those of the coral's environment. The method was demonstrated to be robust in identifying similarities and dif-

ferences in the composition of complex microbial communities (16). Average peak numbers found in the respective sample types mirrored the complexity (richness) of their microbial assemblages: while the sediment is commonly expected to house the most species-rich microflora, seawater bacteria were found to be less diverse than the sediment but richer than the coral samples, which present a rather special environment for bacteria. This was corroborated by nonparametric Kruskal-Wallis ANOVA. The microflora hosted by red *L. pertusa* appeared to be richer than that of white *L. pertusa*, but this difference was insignificant for the given data set.

MDS-aided comparison of T-RFLP profiles demonstrated clear differences between coral, water, and sediment samples (Fig. 1). Since stress values of all ordinations were mostly below 0.10 and never exceeded 0.15, results from dimensional downscaling could be safely used to infer relations between the samples (cf. reference 10). Differences between sample types were again substantiated by both parametric (MANOVA and Duncan's test) and nonparametric (Kruskal-Wallis ANOVA and Mann-Whitney U test) statistics. Separation of the three sample types was not caused by different concentrations of the respective PCR products or due only to water- or sediment-specific T-RFs. It could also be ascribed to a great number of peaks occurring exclusively in the corals (see Table S1 in the supplemental material), denoting a special bacterial community on *L. pertusa*. Consequently, MDS ordination based only on binary (presence-absence) peak data (Fig. 1b) led to the same conclusion regarding sample clustering as ordination based on normalized peak areas (Fig. 1a).

Associations between *L. pertusa* and bacteria varied within the Trondheimsfjord: for both rare and consistent T-RF data, post hoc tests revealed differences between stations 1 ("Tautra") and 2 ("Stokkberneset"), 32.5 km apart from each other. For rare T-RFs (i.e., organisms with more-variable occurrence within *L. pertusa*), differences also manifested between stations 2 and 3 ("Røberg"), which lay only 3.9 km apart but on opposite sides of the bottleneck connecting the seaward fjord basin with the open sea. In contrast, variations between stations 1 and 3 remained insignificant in all analyses, though their distance of 28.7 km was almost as large as that between stations 1 and 2. Accordingly, divergence in bacterial community composition was not related to distances between sampling sites. Results from binary T-RF data suggested that these differences were not caused only by shifts in relative bacterial abundances: though there was no indication that the presence of dominant groups varied between stations, changes in the presence of rare species or groups were significant. Also, Großkurth (24) observed spatial variation in *L. pertusa*-associated bacterial communities from adjacent locations by analysis of denaturing gradient gel electrophoresis patterns and suggested influence of the local environment as an explanation for these inconsistencies. Relative differences in temperature and salinity revealed the presence of slightly warmer and less saline subsurface water at station 1, while no conspicuous divergences of water masses were observed between stations 2 and 3. This does not explain the differences between bacterial associations of coral samples from the three stations. Other physicochemical environmental factors might vary in the sampling region (e.g., current velocity, oxygen saturation, light, nonconservative ions, trace gases, and dissolved and particulate organic matter). In

addition, site-specific macrofaunal associations or differences in the developmental stage of the corals may account for the observed variations (24).

The finding of coral color-dependent bacterial consortia was unexpected and constituted the most intriguing result of this study, warranting detailed investigation by 16S rRNA gene sequence analysis. Divergence of bacterial community composition with coral color was not as evident in T-RFLP as discrepancies between coral and environmental samples but still was statistically significant for relative abundances of dominant T-RFs. Different bacterial species, even from different phyla, can produce the same T-RFs with a given restriction enzyme digestion, which reduces resolution of T-RFLP. Since this was especially the case with dominant T-RFs (data not shown), genetic fingerprinting did not resolve differences among coral color varieties as accurately as the phylogenetic approach.

**Specificity of *L. pertusa*'s bacterial community.** Members of Norwegian *L. pertusa*'s bacterial community are rare in the coral's environment. Notably, this was also true for samples from station 1 ("Tautra"), one of the coral's shallowest occurrences (27) and thus likely to show greater variations in environmental conditions than deeper habitats. Data presented here and by Großkurth (24) displayed spatial variations of coral-associated bacteria within the respective sampling areas. Even more outstanding differences were shown in the present study by comparative analysis of *L. pertusa*-derived DNA sequences from different geographic regions: apart from marginal intersections in the *Alpha*- and *Gammaproteobacteria*, Mediterranean *L. pertusa* hosted bacterial phylotypes (68) that were almost completely different from those in Norwegian specimens. Bottom temperature and salinity of the Central Mediterranean where these corals were sampled are generally around 13.6°C and 38.7 PSU (35). In the Mediterranean, *L. pertusa* actually lives at the limits of its physiological niche, which might be the reason why living deep-water coral banks are generally rare there (14). While temperature and salinity may be physicochemical factors influencing the prokaryotic consortia of *L. pertusa* between the different locations, other factors, such as oxygen concentrations or nutrition, need to be considered as well but are not available from these studies.

*L. pertusa* from the Trondheimsfjord shared many bacterial OTUs with other coral species. By far the most similarities were observed with bacterial lineages from deep-sea gorgonians, so-called "bamboo corals" (Isididae). This family's range of distribution exhibits remarkable parallels to that of *L. pertusa*: it lives from a less than 100-m depth to a more than 4,000-m depth along the Indo-Pacific and Atlantic margins and in the Mediterranean (52) in areas of high hydrodynamic energy and sufficient advection of zooplankton and particulate organic matter as food sources (26). Parallels between microbial inhabitants of *L. pertusa* and symbionts from other warm- and cold-water corals indicate that microbial populations associated with corals are globally distributed as postulated by Bourne and Munn (7). Furthermore, a monophyletic and well-defined cluster within the *Mycoplasma hominis* group (Fig. 5) appears to be exclusively associated with *L. pertusa* and the gorgonian Isididae and *M. elongata*.

This study also reports the first finding of candidate division TM7 in corals. This represents an analogy between coral- and sponge-associated bacteria, for TM7 was recently discovered as

part of the natural microflora of the marine sponge *Chondrilla nucula* (65). Similarities to sponge symbionts were also described for Mediterranean *L. pertusa* by Yakimov et al. (68), who pointed out that specialized microbiota may be important for protecting the coral from pathogens through the production of secondary antibiotics as demonstrated for some sponges. A symbiotic relationship could also be assumed between candidate division TM7 and *L. pertusa*.

In summary, the bacterial community of *L. pertusa* from the Trondheimsfjord cannot be termed "specific" sensu stricto because of their variation with location and host phenotype. However, the parallels to other coral-bacterium associations suggest the existence of certain "cold-water coral-specific" bacterial groups sensu lato.

**Implications for nutrition and health of *L. pertusa*.** In radio-carbon labeling experiments conducted with several species of stony corals, Sorokin (59) showed that the polyps actively incorporate planktonic bacteria. The amount of this bacterial organic carbon assimilated per day was equivalent to 10 to 20% of the carbon content of the polyp's body. Bacteria could thus also provide subsidiary alimentation for *L. pertusa*. By ingesting their own mucus (13), a process that was also observed with *L. pertusa* (45), corals can harvest contained bacteria according to the continuous-flow culture principle. The growth rate of microbes living in the corals' surface mucopolysaccharide layer can be accelerated through elevation of dissolved organic carbon (DOC) levels by an order of magnitude (36). In the Trondheimsfjord, large amounts of DOC accumulate in the euphotic zone during the productive season. Export from the euphotic zone through the sinking and degradation of phytoplankton cells also provides DOC to the deep fjord (6). Though *L. pertusa* is unable to benefit directly from dissolved substances in the water column, members of its bacterial consortia can degrade these sugar compounds and incorporate them into their own biomass, which is then available to the coral. The occurrence of the commonly photoautotrophic cyanobacterium *Synechococcus* sp. in both coral color varieties seems surprising at first glance, since sampling was performed well below the euphotic zone of the Trondheimsfjord. However, if light-independent nitrogen fixation is possible, a diazotrophic symbiosis between *Synechococcus* sp. and *L. pertusa* makes sense. Though the coral may not directly suffer nitrogen limitation from feeding on zooplankton, utilization of organic compounds from the water column by its bacterial inhabitants could require a supplementary source of nitrogen, since exported organic matter is known to be nitrogen depleted. Many *L. pertusa*-associated bacterial groups can catabolize cellulose from phytoplankton that was ingested either through mucus entrapment or as part of the diet of the coral's prey. Even the chitin in the exoskeleton of prey crustaceans can be degraded by *Vibrio*, *Clostridiaceae*, probably *Rubritalea* sp., and most notably by the dominant *Rhodobacteraceae*. This offers another significant contribution to the carbon and nitrogen budget (2) of the coral holobiont. Almost all *Alphaproteobacteria* occurring in Norwegian *L. pertusa* can exploit dimethylsulfoniopropionate (DMSP) or its derivatives (e.g., see reference 69). DMSP is an osmoprotectant produced in high concentrations by marine phytoplankton. The substance and its derivatives are likely to occur in considerable amounts in highly productive coastal regions and fjords, such

as the Trondheimsfjord. The mentioned alphaproteobacteria are regarded as playing an important role in the cycling of these organic sulfur compounds (50). Two OTUs within the gammaproteobacteria showed closest relatedness to endosymbionts of deep-sea mussels colonizing hydrothermal vents. These organisms obviously constitute novel thiotrophs exclusively associated with the red color variety of *L. pertusa*. They might utilize reduced sulfur compounds produced by decomposition of DMSP or sulfur-containing amino acids. Interestingly, relatedness of bacteria from Mediterranean *L. pertusa* to microbes from hydrocarbon seep or hydrothermal sediments (Fig. 4) suggests that they too are involved in metabolizing reduced sulfur compounds. This in turn implies that although Mediterranean corals host different bacterial groups owing to the special environmental conditions, these groups occupy ecological niches connected to sulfur cycling similar to those of microbes in Norwegian *L. pertusa*.

Several bacterial groups observed in Norwegian *L. pertusa* (*Rhodobacteraceae*, *Rhodospirillaceae*, *Vibrio*, *Propionibacterium*, *Planctomyces*, and *Clostridiaceae*) can tolerate or even strictly require anaerobic conditions. Finding sequences closely related to those of strict and facultative anaerobic *Archaea* on coral surface microlayers led Kellogg (33) to hypothesize that anaerobic microniches may exist in the mucus of tropical reef corals. Anthozoan polyps and colonies are in fact diffusion limited in their oxygen consumption even under well-stirred, air-saturated conditions (57). Contraction of the polyps enhances hypoxia, thus favoring anaerobic metabolism in the gastral cavity (40). Observations on aquarium-reared *L. pertusa* showed that its polyps can stay retracted for 3 weeks and longer (45) and can also retract after feeding for up to several days (A. Form, personal communication). This implies that hypoxia occurs in *L. pertusa*'s polyps and, as a consequence, fermentation may occur in the gastral cavity and contribute to the nutrition of this coral. The above-mentioned bacterial groups appear to constitute a specialized community that profits from further degrading end products of the coral's own anaerobic metabolism.

The genus *Shigella* was found on both red and white corals. A closely related organism has also been identified on the scleractinian coral *P. meandrina* (Speck et al., unpublished), and another scleractinian, *Acropora palmata*, shows antibiotic activity against this bacterium (51). It thus cannot be ruled out that *Shigella* sp. affects stony corals as a potential pathogen. Likewise, the genus *Vibrio* was found on *L. pertusa* and on *P. damicornis* (7). While *Vibrio* appears to be a common part of coral microflora (e.g., see reference 38), the genus holds many pathogenic species, some of which are agents of coral diseases (e.g., see reference 3). Yet all specimens of *L. pertusa* analyzed in the present study were apparently healthy, as were the specimens of *P. damicornis* (7). Consequently, *Vibrio* sp. found in both coral species may be an opportunistic pathogen constituting a normal component of the healthy coral microbiota until environmental or physiological factors trigger a pathogenic response (7). The same might hold for *Chryseobacterium* species (*Bacteroidetes*) and *Staphylococcus* species (*Firmicutes*) that were also found in corals: clone HKT72 (accession no. DQ188008) from *Porites* species (30) was identified as uncultured *Chryseobacterium* found in diseased aquatic animals (4). The role of the genus *Staphylococcus*, also observed on *P.*

*damicornis* (7), as a potential coral pathogen was recently discussed (15). The direct negative effect of ocean acidification by anthropogenic CO<sub>2</sub> on the calcification process in cold-water corals has already been recognized (48). But shifts in both pH and temperature can also threaten these animals indirectly through detrimental responses of their bacterial microflora: coral-pathogenic *Vibrio* becomes virulent only at higher water temperatures (e.g., see reference 3). One must be apprehensive of the possibility that bacteria in *L. pertusa* exhibit a pathogenic potential that may likewise be stimulated by a temperature rise or pH changes. Resulting disruption of the balance between the coral and its associated microbiota (even if they are harmless under natural circumstances) can trigger coral mortality as well (36). As a caveat, evidence for the suggested bacterial functions implicated in coral nutrition and health has yet to be provided by culture experiments and/or culture-independent methods, such as verification of functional genes.

**Bacterial community composition and distribution of *L. pertusa*.** The finding of coral color-dependent variations in the bacterial consortia of *L. pertusa* also imposes a question about the cause of the observed differences in bacterial community composition of the two coral phenotypes. Mucus-mediated selection of bacterial symbionts was shown for the scleractinian coral *Acropora palmata*, suggesting the coral mucus plays a role in the structuring of beneficial coral-associated microbial communities (51). Selection of certain bacterial groups by antibiotic or growth-stimulating coral metabolites was also demonstrated for *L. pertusa* (24). Color-related differences in bacterial community composition thus imply that white and red *L. pertusa* colonies produce different microbiologically active substances that lead to color-specific selection of certain bacterial groups over others.

To our knowledge, no investigations have been made so far on the nature of the two phenotypes of *L. pertusa*. It is not even known whether they are genetically or environmentally controlled (45). Both color varieties of *L. pertusa* were found growing entwined at all stations in the Trondheimsfjord, so divergence in their bacterial composition cannot be explained by spatial separation. In contrast, our personal observations and those of other researchers imply that *L. pertusa*'s white color variety occurs more frequently along the northeast Atlantic continental margin than the red one. What does the white coral phenotype cause to be more common than the red one? The dominance of *Rhodobacteraceae* in white corals might be the reason: by drawing energy from sulfur oxidation, these bacteria can exploit even small amounts of organic material as carbon sources. Because of this mixotrophy, *Rhodobacteraceae* are more flexible than obligate species (58) and can also be highly productive under conditions of moderate carbon supply. White *L. pertusa* could thus grow in deeper regions of the continental shelf, where less organic material is available from the water column than is the case for shallow off-coast and fjord habitats. Indeed, the deeper cold-water reefs along the southern and central parts of the northeast Atlantic continental margin comprise exclusively white *L. pertusa* (A. Freiwald, personal communication).

#### ACKNOWLEDGMENTS

We are deeply indebted to J. A. Snelli and the staff of the Trondhjem Biological Station, the crew of R/V "Vita," and E. Breitbarth for their

help in collecting the coral samples. T-RFLP analyses were enabled by the generous donation of GeneScan software by K. Heidorn (Institute for Hematopathology, Kiel University Hospital) and the permission of J. F. Imhoff's work group (IFM-GEOMAR) to use their facilities. Sequencing services were provided by A. Dietsch and M. Friskovec (Institute for Clinical Molecular Biology, Kiel University Hospital). Many thanks go to V. Thiel (IFM-GEOMAR) for her constructive critique of the methodology and contents of the thesis this report is based on.

This research was part of the "Moundforce" project (DU/29/35-1) of the German Research Foundation (DFG) and received cofinancing for cruises through the Leibniz award (DU/29/33), Kiel University.

#### REFERENCES

- Altschul, S. F., W. Gish, W. Miller, E. W. Myers, and D. J. Lipman. 1990. Basic local alignment search tool. *J. Mol. Biol.* **215**:403–410.
- Aluwihare, L. I., D. J. Repeta, S. Pantoja, and C. G. Johnson. 2005. Two chemically distinct pools of organic nitrogen accumulate in the ocean. *Science* **308**:1007–1010.
- Ben-Haim, Y., F. L. Thompson, C. C. Thompson, M. C. Cnockaert, B. Hoste, J. Swings, and E. Rosenberg. 2003. *Vibrio coralliilyticus* sp. nov., a temperature-dependent pathogen of the coral *Pocillopora damicornis*. *Int. J. Syst. Evol. Microbiol.* **53**:309–315.
- Bernardet, J. F., M. Vancanneyt, O. Matte-Tailliez, L. Grisez, P. Tailliez, C. Bizet, M. Nowakowski, B. Kerouault, and J. Swings. 2005. Polyphasic study of *Chryseobacterium* strains isolated from diseased aquatic animals. *Syst. Appl. Microbiol.* **28**:640–660.
- Bond, P. L., P. Hugenholtz, J. Keller, and L. L. Blackall. 1995. Bacterial community structures of phosphate-removing and non-phosphate-removing activated sludges from sequencing batch reactors. *Appl. Environ. Microbiol.* **61**:1910–1916.
- Børshem, K. Y., S. M. Mykkestad, and J.-A. Snelli. 1999. Monthly profiles of DOC, mono- and polysaccharides at two locations in the Trondheimsfjord (Norway) during two years. *Mar. Chem.* **63**:255–272.
- Bourne, D. G., and C. B. Munn. 2005. Diversity of bacteria associated with the coral *Pocillopora damicornis* from the Great Barrier Reef. *Environ. Microbiol.* **7**:1162–1174.
- Brosius, J., T. J. Dull, D. D. Sleeter, and H. F. Noller. 1981. Gene organization and primary structure of a ribosomal operon from *Escherichia coli*. *J. Mol. Biol.* **148**:107–127.
- Bythell, J. C., M. R. Barer, R. P. Cooney, J. R. Guest, A. G. O'Donnell, O. Pantos, and M. D. A. Le Tissier. 2002. Histopathological methods for the investigation of microbial communities associated with disease lesions in reef corals. *Lett. Appl. Microbiol.* **34**:359–364.
- Clarke, K. R. 1993. Nonparametric multivariate analyses of changes in community structure. *Aust. Ecol.* **18**:117–143.
- Cole, J. R., B. Chai, R. J. Farris, Q. Wang, A. S. Kulam-Syed-Mohideen, D. M. McGarrell, A. M. Bandela, E. Cardenas, G. M. Garrity, and J. M. Tiedje. 2007. The Ribosomal Database Project (RDP-II): introducing myRDP Space and quality controlled public data. *Nucleic Acids Res.* **35**:D169–D172.
- Cole, J. R., B. Chai, T. L. Marsh, R. J. Farris, Q. Wang, S. A. Kulam, S. Chandra, D. M. McGarrell, T. M. Schmidt, G. M. Garrity, and J. M. Tiedje. 2003. The Ribosomal Database Project (RDP-II): previewing a new autoaligner that allows regular updates and the new prokaryotic taxonomy. *Nucleic Acids Res.* **31**:442–443.
- Coles, S. L., and R. Strathmann. 1973. Observations on coral mucus 'flocs' and their potential trophic significance. *Limnol. Oceanogr.* **18**:673–678.
- Delibrias, G., and M. Taviani. 1985. Dating the death of Mediterranean deep-sea scleractinian corals. *Mar. Geol.* **62**:175–180.
- Dinsdale, E. A., O. Pantos, S. Smruga, R. A. Edwards, F. Angly, L. Wegley, M. Hatay, D. Hall, E. Brown, M. Haynes, L. Krause, E. Sala, S. A. Sandin, R. V. Thurber, B. L. Willis, F. Azam, N. Knowlton, and F. Rohwer. 2008. Microbial ecology of four coral atolls in the Northern Line Islands. *PLoS ONE* **3**:e1584.
- Dunbar, J. M., L. O. Ticknor, and C. R. Kuske. 2000. Assessment of microbial diversity in four southwestern United States soils by 16S rRNA gene terminal restriction fragment analysis. *Appl. Environ. Microbiol.* **66**:2943–2950.
- Eder, W., L. L. Jahnke, M. Schmidt, and R. Huber. 2001. Microbial diversity of the brine-seawater interface of the Kebrüt Deep, Red Sea, studied via 16S rRNA gene sequences and cultivation methods. *Appl. Environ. Microbiol.* **67**:3077–3085.
- Felsenstein, J. 1989. Phylip—Phylogeny Inference Package (version 3.2). *Cladistics* **5**:164–166.
- Fosså, J. H., P. B. Mortensen, and D. M. Furevik. 2002. The deep-water coral *Lophelia pertusa* in Norwegian waters: distribution and fishery impacts. *Hydrobiologia* **471**:1–12.
- Frasca, S., Jr., E. S. Weber, H. Urquhart, X. F. Liao, M. Gladd, K. Cecchini, P. Hudson, M. May, R. J. Gast, T. S. Gorton, and S. J. Geary. 2005. Isolation and characterization of *Mycoplasma sphenisci* sp. nov. from the choana of an

- aquarium-reared jackass penguin (*Spheniscus demersus*). *J. Clin. Microbiol.* **43**:2976–2979.
21. **Freiwald, A.** 1998. Geobiology of *Lophelia pertusa* (Scleractinia) reefs in the North Atlantic. Habilitation thesis. Universität Bremen, Bremen, Germany.
  22. **Freiwald, A., R. Henrich, and J. Paetzold.** 1997. Anatomy of a deep-water coral reef mound from Stjærnsund, West Finnmark, northern Norway, p. 141–162. *In* N. P. James and A. D. Clarke Jonathan (ed.), *Cool-water carbonates*, vol. 56. SEPM (Society for Sedimentary Geology), Tulsa, OK.
  23. **Gärtner, A., J. Wiese, and J. F. Imhoff.** 2008. *Amphritea atlantica* gen. nov., sp. nov., a gammaproteobacterium from the Logatchev hydrothermal vent field. *Int. J. Syst. Evol. Microbiol.* **58**:34–39.
  24. **Großkurth, A. K.** 2007. Analysis of bacterial community composition on the cold-water coral *Lophelia pertusa* and antibacterial effects of coral extracts. Diploma thesis. Carl von Ossietzky Universität, Oldenburg, Germany.
  25. **Guindon, S., and O. Gascuel.** 2003. A simple, fast, and accurate algorithm to estimate large phylogenies by maximum likelihood. *Syst. Biol.* **52**:696–704.
  26. **Heikoop, J. M., D. D. Hickmott, M. J. Risk, C. K. Shearer, and V. Atudorei.** 2002. Potential climate signals from the deep-sea gorgonian coral *Primnoa resedaeformis*. *Hydrobiologia* **471**:117–124.
  27. **Hovland, M., and M. J. Risk.** 2003. Do Norwegian deep-water coral reefs rely on seeping fluids? *Mar. Geol.* **198**:83–96.
  28. **Huber, T., G. Faulkner, and P. Hugenholtz.** 2004. Bellerophon: a program to detect chimeric sequences in multiple sequence alignments. *Bioinformatics* **20**:2317–2319.
  29. **Jacobson, P.** 1983. Physical oceanography of the Trondheimsfjord. *Geophys. Astrophys. Fluid Dyn.* **26**:3–26.
  30. **Kapley, A., S. Siddiqui, K. Misra, S. Ahmad, and H. Purohit.** 2007. Preliminary analysis of bacterial diversity associated with the *Porites* coral from the Arabian Sea. *World J. Microbiol. Biotechnol.* **23**:923–930.
  31. **Kato, Y., M. Asahara, D. Arai, K. Goto, and A. Yokota.** 2005. Reclassification of *Methylobacterium chloromethanicum* and *Methylobacterium dichloromethanicum* as later subjective synonyms of *Methylobacterium extorquens* and of *Methylobacterium lusitanum* as a later subjective synonym of *Methylobacterium rhodesianum*. *J. Gen. Appl. Microbiol.* **51**:287–299.
  32. **Keane, T. M., C. J. Creevey, M. M. Pentony, T. J. Naughton, and J. O. McInerney.** 2006. Assessment of methods for amino acid matrix selection and their use on empirical data shows that ad hoc assumptions for choice of matrix are not justified. *BMC Evol. Biol.* **6**:29.
  33. **Kellogg, C. A.** 2004. Tropical *Archaea*: diversity associated with the surface microlayer of corals. *Mar. Ecol. Prog. Ser.* **273**:81–88.
  34. **Kelman, D., A. Kushmaro, Y. Kashman, Y. Loya, and Y. Benayahu.** 1998. Antimicrobial activity of a Red Sea soft coral, *Parerythropodium fulvum*: reproductive and developmental considerations. *Mar. Ecol. Prog. Ser.* **169**:87–95.
  35. **Klein, B., W. Roether, B. B. Manca, D. Bregant, V. Beitzel, V. Kovacevic, and A. Luchetta.** 1999. The large deep water transient in the eastern Mediterranean. *Deep-Sea Res. Part I* **46**:371–414.
  36. **Kline, D. I., N. M. Kuntz, M. Breitbart, N. Knowlton, and F. Rohwer.** 2006. Role of elevated organic carbon levels and microbial activity in coral mortality. *Mar. Ecol. Prog. Ser.* **314**:119–125.
  37. **Knowlton, N., and F. Rohwer.** 2003. Multispecies microbial mutualisms on coral reefs: the host as a habitat. *Am. Nat.* **162**:S51–S62.
  38. **Koren, O., and E. Rosenberg.** 2006. Bacteria associated with mucus and tissues of the coral *Oculina patagonica* in summer and winter. *Appl. Environ. Microbiol.* **72**:5254–5259.
  39. **Kulikova, T., P. Aldebert, N. Althorpe, W. Baker, K. Bates, P. Browne, A. van den Broek, G. Cochrane, K. Duggan, R. Eberhardt, N. Faruque, M. Garcia-Pastor, N. Harte, C. Kanz, R. Leinonen, Q. Lin, V. Lombard, R. Lopez, R. Mancuso, M. McHale, F. Nardone, V. Silventoinen, P. Stoehr, G. Stoesser, M. A. Tuli, K. Tzouvara, R. Vaughan, D. Wu, W. Zhu, and R. Apweiler.** 2004. The EMBL Nucleotide Sequence Database. *Nucleic Acids Res.* **32**:D27–D30.
  40. **Levy, O., L. Mizrahi, N. E. Chadwick-Furman, and Y. Achituv.** 2001. Factors controlling the expansion behavior of *Favia favius* (Cnidaria: Scleractinia): effects of light, flow, and planktonic prey. *Biol. Bull.* **200**:118–126.
  41. **Liu, W. T., T. L. Marsh, H. Cheng, and L. Forney.** 1997. Characterization of microbial diversity by determining terminal restriction fragment length polymorphisms of genes encoding 16S rRNA. *Appl. Environ. Microbiol.* **63**:4516–4522.
  42. **Ludwig, W., O. Strunk, R. Westram, L. Richter, H. Meier, Yadhukumar, A. Buchner, T. Lai, S. Steppi, G. Jobb, W. Forster, I. Brettske, S. Gerber, A. W. Ginhart, O. Gross, S. Grumann, S. Hermann, R. Jost, A. König, T. Liss, R. Lussmann, M. May, B. Nonhoff, B. Reichel, R. Strehlow, A. Stamatakis, N. Stuckmann, A. Vilbig, M. Lenke, T. Ludwig, A. Bode, and K.-H. Schleifer.** 2004. ARB: a software environment for sequence data. *Nucleic Acids Res.* **32**:1363–1371.
  43. **Lukow, T., P. F. Dunfield, and W. Liesack.** 2000. Use of the T-RFLP technique to assess spatial and temporal changes in the bacterial community structure within an agricultural soil planted with transgenic and non-transgenic potato plants. *FEMS Microbiol. Ecol.* **32**:241–247.
  44. **McKinness, Z. P., and C. M. Cavanaugh.** 2005. The ubiquitous mussel: *Bathymodiolus* aff. *brevior* symbiosis at the Central Indian Ridge hydrothermal vents. *Mar. Ecol. Prog. Ser.* **295**:183–190.
  45. **Mortensen, P. B.** 2001. Aquarium observations on the deep-water coral *Lophelia pertusa* (L., 1758) (Scleractinia) and selected associated invertebrates. *Ophelia* **54**:83–104.
  46. **Nercessian, O., Y. Fouquet, C. Pierre, D. Prieur, and C. Jeanthon.** 2005. Diversity of bacteria and archaea associated with a carbonate-rich metalliferous sediment sample from the Rainbow vent field on the Mid-Atlantic Ridge. *Environ. Microbiol.* **7**:698–714.
  47. **Noé, S. U., J. Titschack, A. Freiwald, and W.-C. Dullo.** 2005. From sediment to rock: diagenetic processes of hardground formation in deep-water carbonate mounds of the NE Atlantic. *Facies* **52**:183–208.
  48. **Orr, J. C., V. J. Fabry, O. Aumont, L. Bopp, S. C. Doney, R. A. Feely, A. Gnanadesikan, N. Gruber, A. Ishida, F. Joos, R. M. Key, K. Lindsay, E. Maier-Reimer, R. Matear, P. Monfray, A. Mouchet, R. G. Najjar, G.-K. Plattner, K. B. Rodgers, C. L. Sabine, J. L. Sarmiento, R. Schlitzer, R. D. Slater, I. J. Totterdell, M.-F. Weirig, Y. Yamanaka, and A. Yool.** 2005. Anthropogenic ocean acidification over the twenty-first century and its impact on calcifying organisms. *Nature* **437**:681–686.
  49. **Peek, A. S., R. A. Feldman, R. A. Lutz, and R. C. Vrijenhoek.** 1998. Cospeciation of chemoautotrophic bacteria and deep sea clams. *Proc. Natl. Acad. Sci. USA* **95**:9962–9966.
  50. **Penn, K., D. Wu, J. A. Eisen, and N. L. Ward.** 2006. Characterization of bacterial communities associated with deep-sea corals on Gulf of Alaska seamounts. *Appl. Environ. Microbiol.* **72**:1680–1683.
  51. **Ritchie, K. B.** 2006. Regulation of microbial populations by coral surface mucus and mucus-associated bacteria. *Mar. Ecol. Prog. Ser.* **322**:1–14.
  52. **Roark, E. B., T. P. Guilderson, S. Flood-Page, R. B. Dunbar, B. L. Ingram, S. J. Fallon, and M. McCulloch.** 2005. Radiocarbon-based ages and growth rates of bamboo corals from the Gulf of Alaska. *Geophys. Res. Lett.* **32**:L04606.
  53. **Rogers, A. D.** 1999. The biology of *Lophelia pertusa* (Linnaeus 1758) and other deep-water reef-forming corals and impacts from human activities. *Int. Rev. Hydrobiol.* **84**:315–406.
  54. **Rohwer, F., V. Seguritan, F. Azam, and N. Knowlton.** 2002. Diversity and distribution of coral-associated bacteria. *Mar. Ecol. Prog. Ser.* **243**:1–10.
  55. **Sakshaug, E., and S. M. Mykkestad.** 1973. Studies on the phytoplankton ecology of the Trondheimsfjord. III. Dynamics of phytoplankton blooms in relation to environmental factors, bioassay experiments and parameters for the physiological state of the populations. *J. Exp. Mar. Biol. Ecol.* **11**:157–188.
  56. **Schöttner, S., C. Wild, A. Ramette, F. Hoffmann, and A. Boetius.** 2008. Habitat differentiation by the cold-water coral *Lophelia pertusa* (Scleractinia) governs bacterial diversity. *Geophys. Res. Abstr.* **10**:EGU2008-A-10666. doi:1607-7962/gra/EGU2008-A-10666.
  57. **Shick, J. M.** 1990. Diffusion limitation and hyperoxic enhancement of oxygen consumption in zooxanthellate sea anemones, zoanthids, and corals. *Biol. Bull.* **179**:148–158.
  58. **Sorokin, D. Y., T. P. Tourova, and G. Muyzer.** 2005. *Citricella thiooxidans* gen. nov., sp. nov., a novel lithoheterotrophic sulfur-oxidizing bacterium from the Black Sea. *Syst. Appl. Microbiol.* **28**:679–687.
  59. **Sorokin, Y. I.** 1973. On the feeding of some scleractinian corals with bacteria and dissolved organic matter. *Limnol. Oceanogr.* **18**:380–385.
  60. **Squires, D. F.** 1959. Deep sea corals collected by the Lamont Geological Observatory. I. Atlantic corals. *Am. Museum Novitates* **1965**:1–42.
  61. **Stackebrandt, E., and B. M. Goebel.** 1994. A place for DNA-DNA reassociation and 16S ribosomal-RNA sequence-analysis in the present species definition in bacteriology. *Int. J. Syst. Bacteriol.* **44**:846–849.
  62. **Strømgren, T.** 1971. Vertical and horizontal distribution of *Lophelia pertusa* (Linnaeus) in Trondheimsfjorden on the west coast of Norway. *Det Kongelige Norske Videnskabers Selskab Forhandling* **6**:1–9.
  63. **Suzuki, Y., F. Inagaki, K. Takai, K. H. Neelson, and K. Horikoshi.** 2004. Microbial diversity in inactive chimney structures from deep-sea hydrothermal systems. *Microb. Ecol.* **47**:186–196.
  64. **Teske, A., T. Brinkhoff, G. Muyzer, D. P. Moser, J. Rethmeier, and H. W. Jannasch.** 2000. Diversity of thiosulfate-oxidizing bacteria from marine sediments and hydrothermal vents. *Appl. Environ. Microbiol.* **66**:3125–3133.
  65. **Thiel, V., S. Leininger, R. Schmaljohann, F. Brümmer, and J. F. Imhoff.** 2007. Sponge-specific bacterial associations of the Mediterranean sponge *Chondrilla nucula* (Demospongiae, Tetractinomorpha). *Microb. Ecol.* **54**:101–111.
  66. **Thiel, V., S. C. Neuling, T. Staufenberger, R. Schmaljohann, and J. F. Imhoff.** 2007. Spatial distribution of sponge-associated bacteria in the Mediterranean sponge *Tethya aurantium*. *FEMS Microbiol. Ecol.* **59**:47–63.
  67. **Ueno, Y., S. Haruta, M. Ishii, and Y. Igarashi.** 2001. Microbial community in anaerobic hydrogen-producing microflora enriched from sludge compost. *Appl. Microbiol. Biotechnol.* **57**:555–562.
  68. **Yakimov, M. M., S. Cappello, E. Crisafi, A. Tursi, A. Savini, C. Corselli, S. Scarfi, and L. Giuliano.** 2006. Phylogenetic survey of metabolically active microbial communities associated with the deep-sea coral *Lophelia pertusa* from the Apulian Plateau, central Mediterranean Sea. *Deep-Sea Res. Part I* **53**:62–75.
  69. **Yoch, D. C.** 2002. Dimethylsulfoniopropionate: its sources, role in the marine food web, and biological degradation to dimethylsulfide. *Appl. Environ. Microbiol.* **68**:5804–5815.